

**Title**

Synthesis and characterization of lignin-based cationic dye-flocculant

**Authors**

Masaru Kajihara, Dan Aoki\*, Yasuyuki Matsushita, Kazuhiko Fukushima

Graduate School of Bioagricultural Sciences, Nagoya University, Chikusa-ku, Nagoya 464-8601,  
Japan

E-mail: daoki@agr.nagoya-u.ac.jp

**Abstract**

Kraft lignin derivatives having cationic poly 2-(trimethylamino)ethyl methacrylate side chains were synthesized and their property as dye-flocculant was investigated. Lignin-based flocculants having 3 types of side chain densities and 3 types of side chain lengths were synthesized by esterification of the lignin hydroxyl groups with bromoisobutyryl groups, atom transfer radical polymerization using 2-(dimethylamino)ethyl methacrylate, and quaternization of the amino groups. Dye removal test was performed using three organic dyes and the obtained lignin-based flocculants. The results indicated that the density and the length of the side chains obviously affected the flocculation behavior. When the flocculants containing the same nitrogen amount were compared, the flocculation performance was improved with the increase of the side chain length within the samples having low and middle side chain densities. In the case of the samples having high side chain density, the most efficient sample was not the sample having the longest side chain. Most of the lignin-based flocculants removed dyes more efficiently than the poly 2-(trimethylamino)ethyl methacrylate homopolymer. From these results, it was suggested that lignin has a potential character as the core molecule to design the high-efficient dye-flocculant.

## Introduction

Dyes are used as colorants in the textile, leather, paper, plastic, and food process industries. Annually, more than 700,000 t of dyes are produced, and it is estimated that 10–15 % of them are discharged in effluent.<sup>1,2</sup> Effluent containing dyes pollute the aquatic environment such as lakes and rivers, resulting in the reduction of light penetration. As a result, photosynthesis and growth of aquatic plants are obstructed.<sup>3–5</sup> What is worse, most of dyes may adversely affect health of not only aquatic organisms but also humans due to their toxicity and carcinogenicity.<sup>4,6</sup> Therefore, dyes should be removed as much as possible from effluent.

Various methods such as coagulation/flocculation,<sup>7–9</sup> adsorption,<sup>10–12</sup> filtration,<sup>13</sup> oxidation,<sup>14,15</sup> and biological treatment<sup>14,16</sup> are examined to remove dyes. Coagulation/flocculation process is one of the most effective methods in terms of low cost, easy operation, and energy saving.<sup>17</sup> The advantage of this method is that effluent is purified by direct removal of dye molecules, not by partially decomposition which may generate harmful toxic compounds.<sup>18</sup> At present, inorganic flocculants including ferric salt, aluminum salt and magnesium salt, and organic flocculants such as synthetic polymers are used.<sup>19–21</sup> However, there are drawbacks in the use of them; the relation between residual aluminum flocculants and Alzheimer has reported.<sup>22,23</sup> Thus, organic-based high-efficient dry-flocculant is desired.

Lignin is the second most abundant natural polymer after cellulose. Lignin has an aromatic backbone with hydroxyl groups which can be chemically modified. However, the complex and heterogeneous structure of lignin makes its commercial use difficult. Most of technical lignins collected in the pulping process are burned for thermal recycling.<sup>24</sup> A few percent of technical lignins possessing specific functional groups, such as liginosulfonate, are used as biomaterials.<sup>25–27</sup> Recently, various researches on the effective utilization of commercially unused technical lignins have reported<sup>28</sup>; for example, fillers,<sup>29</sup> fertilizers,<sup>30</sup> adsorbents,<sup>31</sup> bioplastics,<sup>32</sup> carbon fibers,<sup>33</sup> and composites.<sup>34</sup>

There are also studies on flocculants derived from technical lignins taking advantage of its aromatic hydrophobicity. Lignin derivatives having acrylamide-graft chain,<sup>35</sup> hexane-diamine side-chain,<sup>36</sup> and sulfomethyl group<sup>37</sup> were prepared and their flocculating properties were studied. These researches mainly focus on the correlation between the charge density of the flocculants and the flocculation behavior. Although the steric property of the flocculant should also be one of the important factors for the flocculation behavior, their detailed correlation was not appreciated enough. To develop more effective lignin-based polymeric flocculants, the basic knowledge of the correlation between the chemical structures of flocculants and the flocculation behavior is needed.

In this study, lignin-based flocculants having 3 types of side chain densities and 3 types of side chain lengths were synthesized by esterification of the lignin hydroxyl groups with bromoisobutyryl groups, atom transfer radical polymerization<sup>38,39</sup> using 2-(dimethylamino)ethyl methacrylate (DMAEMA), and quaternization of the amino groups. The length and density of the graft chain was estimated as their structural parameters. Dye-flocculating property of the resultant lignin derivatives having cationic poly 2-(trimethylamino)ethyl methacrylate (PTMAEMA) side chains was

investigated concerning with their structural parameters. As a result, most of the lignin-based flocculants removed dyes more efficiently than the PTMAEMA homopolymer and it was suggested that lignin has a potential character as the core molecule to design the high-efficient dye-flocculant. Thus obtained correlation between the chemical structures of flocculants and the flocculation behavior might be useful information not only to design high efficient flocculants but also to enhance the efficient use of lignin-derived materials.

## Methods

### 1. Materials

Kraft lignin (KL, lignin alkali, 370959-500G), Remazol Brilliant Blue R (RBB), Direct Red 23 (DR), Aluminum oxide (activated, neutral, Brockmann I), Aluminum oxide (activated, basic, Brockmann I) were purchased from Sigma-Aldrich Co. LLC, USA. Pyridine, acetyl chloride (AcCl), nitric acid, copper bromide(I) (CuBr), tetrahydrofuran (THF) and other reagents were purchased from KISHIDA CHEMICAL Co., Ltd., Japan. 2-Bromoisobutyryl bromide (BrBBr), 2-(dimethylamino)ethyl methacrylate (DMAEMA), ethyl 2-bromoisobutyrate (EtBBr), 5-bromovanillin were purchased from Tokyo Chemical Industry Co., Ltd., Japan. Acid Black 1 (AB), was purchased from Kanto Chemical Co., Inc., Japan. *N,N*-dimethylacetamide (DMAc), *N,N,N',N'',N'''*-pentamethyldiethylenetriamine (PMDETA), bromophenol blue, diphenylcarbazone, and mercury(II) nitrate were purchased from Wako Pure Chemical Industries, Ltd., Japan. Sodium 3-trimethylsilylpropionate-2,2,3,3,-*d*<sub>4</sub> (TSP) was purchased from MERCK&CO., INC., USA.

Lignin alkali was used after drying *in vacuo* at 40°C overnight. DMAEMA was used after purification using basic aluminum oxide to remove polymerization inhibitors. CuBr was used after washing by acetic acid, ethanol, and diethyl ether and drying *in vacuo* at room temperature. Other reagents were used without further purification.

### 2. Synthesis of lignin initiators (KLBrB)

DMAc (50 mL), KL (2.50 g), and pyridine (6.16 mL) were added into a flask. Esterification was carried out by the attack reagent which has a designated ratio of BrBBr and AcCl for 6 hours at 40 °C in a nitrogen atmosphere. After the reaction, the reaction mixture was reprecipitated in an excess amount of methanol. The product KLBrB was purified by dissolving in chloroform and reprecipitating into methanol and then filtering. Finally, KLBrB was dried *in vacuo* at 40 °C.

The molar quantity of bromine in KLBrB sample was determined by the flask combustion method followed by the titration of mercury(II) nitrate<sup>40, 41</sup> as follows. The sample (10.0 mg) was wrapped in filter paper and put in a Pt basket. The sample was burned in a combustion flask containing 15 mL H<sub>2</sub>O and fulfilled by oxygen. The sealed flask was kept standing for an hour to finish the bromine absorption to H<sub>2</sub>O. Aqueous solution of 0.01 % bromophenol blue (2.5 mL) was added into the absorbing water. The pH of the solution adjusted to 3.6 using aqueous solutions of 0.1 N NaOH and 0.1 N HNO<sub>3</sub>. After an addition of aqueous solution of 0.2 % diphenylcarbazone, the Br molar quantities was titrated by 0.005 N mercury(II) nitrate. The molar amount of KLBrB

were evaluated based on the calibration curve obtained by 5-bromovanillin.

### 3. Synthesis of lignin derivatives with PDMAEMA side chains (KLB-PDMAEMA)

ATRP reaction and quaternization of DMAEMA was performed referring the previous study.<sup>42</sup>  
<sup>43</sup> In this experiment, glass tools were washed by 30 % HNO<sub>3</sub> aqueous solution before use. CuBr (52.5 mg), anisole, DMAEMA (4.57 mL), PMDETA (96.8 μL), and KLBBrB (0.10 g) were added to a three-neck flask in this order under an argon flow at 50 mL/min, and then the mixtures were stirred until KLBBrB dissolved. Then, a dimroth condenser was attached and an argon flow was stopped. ATRP was carried out at 120 °C. Just after polymerization, <sup>1</sup>H NMR measurement for the reaction solution was performed to calculate conversions from peak area ratios of monomers and polymers. The reaction solution was diluted by chloroform to decrease viscosity followed by removal of Cu by neutral aluminum oxide. After removal of chloroform by vacuum concentration, KLB-PDMAEMA was reprecipitated in petroleum ether. KLB-PDMAEMA was purified by dissolving in acetone and reprecipitating into petroleum ether and then filtering. Finally, KLB-PDMAEMA was dried *in vacuo* for 48 h at 40 °C.

### 4. Synthesis of lignin derivatives with PTMAEMA side chains (KLB-PTMAEMA)

KLB-PDMAEMA (0.5 g), distilled water (25 mL), and iodomethane (3 eq/amine) were added into a flask. The quaternization reactions were conducted with the molar ratio of amine:iodomethane = 1:3. Quaternization was carried out for 5 hours at 30 °C in a nitrogen atmosphere. After quaternization, dialysis with distilled water was performed for 3 days, followed by freeze-drying to obtain KLB-PTMAEMA.

### 5. Synthesis of PTMAEMA homopolymer

PDMAEMA homopolymer was synthesized in the same way of KLB-PDMAEMA. CuBr (52.5 mg), anisole (9.14 mL), DMAEMA (4.57 mL), PMDETA (96.8 μL) and EtBBR (54.8 μL) were used. The reaction temperature was 120°C and the reaction time was 72 h.

PTMAEMA homopolymer was prepared in the same way of KLB-PTMAEMA. PDMAEMA homopolymer (0.10 g), distilled water (5.0 mL) and iodomethane (0.12 mL) were used. The reaction temperature was 30°C and the reaction time was 5 h. PTMAEMA was purified by dialysis for 3 days and freeze-dried.

### 6. Measurements

The FT-IR measurement was performed by HORIBA FT-720 (HORIBA, Ltd., Japan) using an attenuated total reflection (ATR) option. The measurement range was 800–4000cm<sup>-1</sup>, the resolution capability was 4 cm<sup>-1</sup>, and the number of scan was 32.

The gel permeation chromatography (GPC) was performed by SPD-20A system (Shimadzu Corporation, Japan) connected with TSK gel α-6000, α-4000, α-2500 sequentially. The flow rate was 1.0 mL/min, the mobile phase was THF with stabilizer, the sample concentration was 0.5 w/v%,

the column temperature was 40 °C, and the reference samples were monodisperse polystyrenes.

The NMR measurement was performed by AVANCE400 (400MHz, Bruker, USA). KLBrB was dissolved in CDCl<sub>3</sub> with 0.03 % TMS. KLB-PDMAEMA and PDMAEMA homopolymer were dissolved in CDCl<sub>3</sub> with 0.03 % TMS. KLB-PTMAEMA and PTMAEMA homopolymer were dissolved in D<sub>2</sub>O with 0.05 w/v% TSP.

The elemental analysis was performed by CHN coder MT-6 (YANACO Co., Ltd., Japan). Each sample was measured twice, and the average value was used.

## 7. Dye removal test

Dye removal tests were carried out at room temperature (25 °C), and Remazol Brilliant Blue R (RBB), Direct Red 23 (DR), and Acid Black 1 (AB) were used as dyes. 100 mg/L of aqueous solution of dyes were prepared, and then 7 mL of the solution was added in a test tube. The amount of nitrogen included in KLB-PTMAEMA was calculated from the results of elemental analysis, and KLB-PTMAEMA solution containing the desired amount of nitrogen was added. After shaking for 10 seconds, the mixed solution was left stationary for 10 minutes, and then centrifuged for 10 minutes at 4000 rpm. After centrifugation, the absorbance of the supernatant was measured by UV-Vis spectrophotometer (V-530, JASCO, Japan). The measurement wavelengths of RBB, DR, and AB were 593 nm, 506 nm, and 618 nm, respectively. The dye concentration of the supernatant was calculated from the calibration curve of each dye. The dye removal efficiency was determined as follow:

$$\text{Dye removal efficiency (\%)} = (C_0 - C) / C_0 \times 100$$

where  $C_0$  and  $C$  are the dye concentrations in solution before and after flocculation, respectively. The experiment was conducted for 3 times.

## Result and Discussion

### 1. Synthesis of KLBrB

Lignin has plural alcoholic and phenolic hydroxyl groups in the molecule. To arrange the side chain density, KL was esterified by the mixed attack reagent containing AcCl and BrBBBr. Bromoisobutyryl group contains Br as an ATRP initiation site, while acetyl group has no halogen. The reaction conditions were summarized in Table 1. The reactions were conducted with BrBBBr only for L100, BrBBBr:AcCl=3:1(mol) for L59, BrBBBr:AcCl=1:1 for L22, and AcCl only for L0 preparation, where the numerical values of the sample code mean the ratio of the Br-containing ester side chain to the total side chains (see below).

The completion of the esterification reaction was confirmed by FT-IR measurements. In Fig. 1,  $\nu$ O-H band at 3400 cm<sup>-1</sup> was disappeared and  $\nu$ C=O band at 1750 cm<sup>-1</sup> arose after the reaction. This change suggests that most of lignin hydroxyl groups were substituted by ester groups. Further examination was performed by <sup>13</sup>C NMR measurements. In <sup>13</sup>C NMR spectra of Fig. 2, L100 and L0 sample showed a signal derived from bromoisobutyryl and acetyl groups, respectively. As for the lignin derivatives esterified by the mixed attack reagent, <sup>13</sup>C NMR spectra of L59 and L22

suggested that they contain both types of side chains.

It should be noted that all of these lignin derivatives were soluble in  $\text{CHCl}_3$ , THF, and toluene. This good solubility should be attributed by the complete esterification of the lignin hydroxyl groups. If we tried to control the Br amount by the esterification degree and left some portion of free hydroxyl groups as they were, the solubility of the sample was quite low. Acetyl groups providing solvent solubility was essential for the following homogeneous reactions and measurements.

To evaluate the specific amount of Br initiation site in the lignin molecule, Br amount was quantified by titration. Further, GPC measurements were carried out. These results were displayed in Table 1. The number of Br per a KLBrB molecule was roughly estimated by multiplying Br amount (mmol/g) by  $M_n$  evaluated by GPC. As a result, Br amount (mol/mol-KLBrB) of the lignin initiator esterified only by BrBBR was 20.5. Although  $M_n$  values were simply the converted values using polystyrene standard, it should be possible to use these values as a guideline of lignin molecules. Average degree of polymerization of the lignin samples ( $DP_L$ ) were calculated as follows:

$$DP_{L100} = (M_n - 20.5 \times [\text{COC}(\text{CH}_3)_2\text{Br}] + 20.5 \times [\text{H}]) / [\text{C}_{10}\text{H}_{11.4}\text{O}_{3.3}\text{S}_{0.14}] = 13.48$$

$$DP_{L0} = (M_n - 20.5 \times [\text{COCH}_3] + 20.5 \times [\text{H}]) / [\text{C}_{10}\text{H}_{11.4}\text{O}_{3.3}\text{S}_{0.14}] = 13.44$$

where  $M_n$  is the number average molecular weight in Table 1, 20.5 is the average number of side chains,  $[\text{COC}(\text{CH}_3)_2\text{Br}]$ ,  $[\text{COCH}_3]$ , and  $[\text{H}]$  are the formula weight of the side chains, and  $[\text{C}_{10}\text{H}_{11.4}\text{O}_{3.3}\text{S}_{0.14}]$  is the formula weight of the structural unit of kraft lignin as reported by Gellerstedt et al.<sup>44,45</sup> From these approximate calculations,  $DP_L$  was estimated as 13.46 in average. Using these values, Br amounts (mol/mol-KLBrB) of the two mixed ester derivatives were also estimated by the following simultaneous equations:

$$\text{Br (mol/mol-KLBrB)} = \text{Br (mmol/g-KLBrB)} \times MW_{\text{calc}}/1000$$

$$MW_{\text{calc}} = 13.46[\text{C}_{10}\text{H}_{11.4}\text{O}_{3.3}\text{S}_{0.14}] - 20.5 \times [\text{H}] + \text{Br (mol/mol-KLBrB)} \times [\text{COC}(\text{CH}_3)_2\text{Br}] + ((20.5 - \text{Br (mol/mol-KLBrB)}) \times [\text{COCH}_3])$$

where Br (mmol/g-KLBrB) was the obtained value by titration as shown in Table 1. As a result, Br (mol/mol-KLBrB) was estimated as 12.02 for L59 and 4.50 for L22. Hereafter, we designate the sample codes of lignin initiators using the Br side chain ratio; e.g., L100, L59, L22, and L0.

## 2. Synthesis of KLB-PTMAEMA and PTMAEMA

By the ATRP reaction starting from the Br initiation site of KLBrB, lignin derivatives having tertiary amino side chains were prepared.  $^1\text{H}$  NMR spectrum of the KLB-PDMAEMA was shown in Fig. 3 with their signal assignments. Average degree of polymerization of side chains (DPs) was calculated using the monomer conversion values as follows:

$$\text{Conversion} = A' / (A + A')$$

$$\text{DPs} = [\text{DMAEMA}]/[\text{Br}] \times \text{Conversion}$$

where  $A$  and  $A'$  are peak areas of the peaks A and A' in Figure 3.

The reaction conditions and the resultant conversion and DPs were summarized in Table 2.

Hereafter, grafted lignin samples are designated with their structural parameter of the Br side chain ratio and the DPs; e.g., L100g39 means that the sample was synthesized from L100 and the DPs was 39.

In Table 2, it was confirmed that the conversion was enhanced by increasing the monomer concentration and the reaction time. However, when the monomer concentration reached at 40 %, gelation occurred during the reaction. Therefore, we set the limit of the monomer concentration as 33 % in this reaction. The polymerizations were conducted with DMAEMA:Br:CuBr:PMDETA = 110:1.50:1.5:1.9 in L100 reaction system, 110:1.05:1.5:1.9 in L59 reaction system, and 110:0.48:1.5:1.9 in L22 reaction system. In Table 2, the conversion decreased with the decrement of the polymerization initiation sites. Focusing on the DPs, however, the DPs increased with the increment of the molar ratios of the monomer to the polymerization initiating site.

Next, KLB-PDMAEMA samples were quaternized by CH<sub>3</sub>I to obtain KLB-PTMAEMA samples. The reaction progress was investigated by <sup>1</sup>H NMR measurements. In Fig. 4, <sup>1</sup>H NMR spectra of L59g52 sample before and after the quaternization reaction was displayed. After the reaction, the signals derived from tertiary amino side chains diminished completely. Consequently, the quaternization reaction was conducted quantitatively in this system. The quaternized samples are indicated using a prefix “q” for the sample code; e.g., L59g52 was converted to qL59g52. As shown in Table 2, lignin-based flocculants having 3 types of side chain densities and 3 types of side chain lengths were successfully synthesized.

Homopolymers of PDMAEMA and PTMAEMA were prepared with the same reaction system using EtBBr as a starting reagent. The resultant DP was estimated as 40 and the sample code was g40 in Table 2. For the next dye removal test, the elemental compositions of these cationic samples were analyzed and summarized in Table 3. The sample having longer DPs had higher N to C ratio. The homopolymer qq40 naturally showed the highest N to C ratio.

### 3. Dye removal property

To investigate dye-flocculating property of the cationic lignin derivatives, dye removal tests were conducted using 3 types of anionic dyes of Remazol Brilliant Blue R (RBB), Direct Red 23 (DR), and Acid Black 1 (AB). The lignin derivatives were added into the dye-solutions. After the dye flocculation, the dye removal efficiency was evaluated by measuring the dye concentration in the supernatant of the mixed solution. Resultant dye removal efficiency based on the molar ratio between cationic quaternary amino groups in the lignin derivatives and the dye were summarized in Fig. 5. Figures 5a, 5b, and 5c are the results of L22 series lignin derivatives for 3 types of dyes. Figures 5d, 5e, 5f and 5g, 5h, 5i are the results of L59 and L100 series lignin derivatives, respectively. The columns at left, center, and right sides are the results for RBB, DR, and AB, respectively. Incidentally, TMAEMA monomer did not show any dye flocculation behavior.

Figure 5a displays three series of plots corresponding to the 3 types of DPs; qL22g94, qL22g37, and qL22g5. As a result, qL22g94 showed the highest dye removal ratio and the lowest molar ratio of nitrogen to dyes. The best condition to remove dyes was 160 % addition to the

solution (98 % removal). If the molar ratio of nitrogen to dyes were higher than the best, the dye removal efficiency drastically decreased probably because of the positive conversion of the solution. qL22g37 exhibited nearly the same molar efficiency but a little bit lower removal ratio than that of qL22g94. In the case of qL22g5, the molar efficiency was lower than the others and the plots shifted to the right (high molar ratio of N to dye).

Figure 5d shows the results of L59 series. The resultant trend was similar with that of L22 series described above; the higher DPs exhibited the higher efficiency. The removal ratio of L59 series were 92–98 %. As for the molar efficiency, L59 series exhibited better results than that of L22 series. Especially, qL59g52 and qL59g30 demonstrated wide-range applicability from the view point of molar efficiency.

With the highest side chain density samples of L100 series, however, the dye removal ability decreased as displayed in Fig. 5g. The applicable ranges were narrower than that of L59 series. Especially, the molar efficiency of the longest DPs sample of qL100g39 obviously decreased from the others. Finally, the results using PTMAEMA homopolymer of qg40 was worse than that of qL100g39. The result means that most of the lignin-based flocculants can remove RBB more efficiently than PTMAEMA homopolymer.

As for DR (Fig. 5b, 5e, and 5h), the lignin-based flocculants having longer side chains showed high removal efficiency in the low (Fig. 5b) and middle (Fig. 5e) side chain density samples. For the high side chain density samples (Fig. 5h), qL100g39 having the longest side chains showed high removal ability but needed high molar ratio to dyes. In the case of AB (Fig. 5c, 5f, and 5i), the general trend was similar with that for RBB and DR. In either case, the homopolymer qg40 was inferior flocculant from the viewpoints of removal ability and molar efficiency as displayed in Fig. 5h and 5i.

From these results, we can conclude that the removal efficiency and the molar efficiency of the cationic lignin-based flocculants for these 3 dyes are under the strong influence of density and length of the side chain. Furthermore, the core-molecule of lignin should have an important role to express the high efficiency. The chemical structure of lignin is an indeterminate because it has plural structural units and bonding patterns. The skeletal structure of lignin is a hydrophobic phenylpropane unit. Each unit might have 1–3 hydroxyl groups and they were esterified in this study. Based on these characters, we assumed that the most of introduced cationic hydrophilic side chains should be turning outward and the whole molecular structure of the lignin-based flocculants would be approximated to a star-shape. Concerning these points, we hypothesized the flocculation mechanism as Fig. 6.

Figure 6 schematically illustrates the flocculation behavior between lignin-based star-shaped cationic flocculants and anionic dyes. The core-molecule of lignin has several cationic graft side chains. Although the actual shape of core-lignin in aqueous solution was not clear in this study, the esterified aromatic skeleton should be hydrophobic and we illustrated it as a particle at the center of the flocculant molecule to make the scheme simple. The side chains should have expanding character in neutral pH because of their intramolecular ionic repulsion which enables the stable

dispersion of the flocculant molecules.<sup>46, 47</sup> When the anionic dyes and the flocculants are mixed in the solution, the electrostatic coupling makes the molecules neutral and decreases their water solubility. Then the hydrophobic interaction between the neutralized molecules forms large agglomerate. In this scheme, if both of the side chain density and length were too high, the inner cationic site might not join the electrostatic coupling because of the steric hindrance. As a result, the molar efficiency of the L100 series should be low (Fig. 5g, 5h, and 5i). With the lower side chain density (L22 and L59 series), longer side chains might contribute both of dye-capture and hydrophobic aggregation.

## Conclusions

In this study, kraft lignin-based star-shaped flocculants having various side chain densities and lengths were successfully synthesized. Their dye flocculating property was investigated and discussed in consideration of their structural properties. In the dye removal test, the lignin-based flocculants could remove 3 dyes more efficiently than PTMAEMA homopolymer. As a result, the potential ability of lignin as a core-molecule of the star-shaped flocculants was demonstrated. The correlation between the chemical structures of the flocculants and the flocculation behavior would be a guiding knowledge to design high efficient flocculants in future. The effect of any other coexisting-chemicals in the waste-water, pH of the system, and the recycling availability of the flocculant should be discussed for further application.

## Acknowledgments

This study was financially supported by the Japan Society for the Promotion of Science KAKENHI (No. 17H03842). The authors thank Analysis and Materials Support Area, Technical Center of Nagoya University for performing elemental analysis.

## References

1. Tian, D., Zhang, X., Lu, C., Yuan, G., Zhang, W. and Zhou, Z. *Cellulose* **2014**, *21*, 473–484.
2. Zhou, K., Zhang, Q., Wang, B., Liu, J., Wen, P., Gui, Z. and Hu, Y. *J. Clean. Prod.* **2014**, *81*, 281–289.
3. Xiong, J., Jiao, C., Li, C., Zhang, D., Lin, H. and Chen, Y. *Cellulose* **2014**, *21*, 3073–3087.
4. Yagub, M. T., Sen, T. K., Afroze, S. and Ang, H. M. *Adv. Colloid Interface Sci.* **2014**, *209*, 172–184.
5. Khraisheha, M. A. M., Al-Ghoutib, M. A., Allenb, S. J. and Ahmad, M. N. *Water Res.* **2005**, *39*, 922–932.
6. Crini, G. *Bioresour. Technol.* **2006**, *97*, 1061–1085.
7. Liang, C.-Z., Sun S.-P., Li, F.-Y., Ong, Y.-K. and Chung, T.-S. *J. Membr. Sci.* **2014**, *469*, 306–315.
8. Verma, A. K., Dash, R. R. and Bhunia, P. *J. Environ. Manage.* **2012**, *93*, 154–168.
9. Zahrim, A. Y., Tizaoui, C. and Hilal, N. *Desalination* **2011**, *266*, 1–16.
10. Batmaz, R., Mohammed, N., Zaman, M., Minhas, G., Berry, R. M. and Tam, K. C. *Cellulose*

**2014**, *21*, 1655–1665.

11. Yagub, M. T., Sen, T. K. and Ang, H. M. *Water Air Soil Pollut* **2012**, *223*, 5267–5282.
12. Rafatullaha, Mohd., Sulaimana, O., Hashima, R. and Ahmad, A. *J. Hazard. Mater.* **2010**, *177*, 70–80.
13. Koyuncu, I. *Desalination* **2002**, *143*, 243–253.
14. Punzi, M., Anbalagan, A., Börner, R. A., Svensson, B.-M., Jonstrup, M. and Mattiasson, B. *Chem. Eng. J.* **2015**, *270*, 290–299.
15. Wang, C., Zhang, Y., Yu, L., Zhang, Z. and Sun, H. *J. Hazard. Mater.* **2013**, *260*, 851–859.
16. Daneshvar, N., Ayazloo, M., Khataee, A. R. and Pourhassan, M. *Bioresour. Technol.* **2007**, *98*, 1176–1182.
17. Cai, T., Li, H., Yang, R., Wang, Y., Li, R., Yang, H., Li, A. and Cheng, R. *Cellulose* **2015**, *22*, 1439–1449.
18. Aboulhassan, M. A., Souabi, S., Yaacoubi, A. and Bauduc, M. *J. Hazard. Mater.* **2006**, *B138*, 40–45.
19. Zhao, Y. X., Gao, B. Y., Shon, H. K., Wang, Y., Kim, J.-H. and Yue, Q. Y. *J. Hazard. Mater.* **2011**, *198*, 70–77.
20. Wang, Y., Gao, B., Yue, Q., Zhan, X., Si, X. and Li, C. *J. Environ. Manage.* **2009**, *91*, 423–431.
21. Li, T., Zhu, Z., Wang, D., Yao, C. and Tang, H. *Powder Technol.* **2006**, *168*, 104–110.
22. Szyguła, A., Guibal, E., Palacín, M. A., Ruiz, M. and Sastre, A. M. *J. Environ. Manage.* **2009**, *90*, 2979–2986.
23. Ndabigengesere, A. and Narasiah, K. S. *Water Res.* **1998**, *32*, 781–791.
24. El Mansouri, N.-E. and Salvadó, J. *Ind. Crop. Prod.* **2007**, *26*, 116–124.
25. Matsushita, Y. *J. Wood Sci.* **2015**, *61*, 230–250.
26. Wang, X. and Zhao, J. *J. Agric. Food Chem.* **2013**, *61*, 3789–3796.
27. Yang, D., Qiu, X., Zhou, M. and Lou, H. *Energy Convers. Manage.* **2007**, *48*, 2433–2438.
28. Ten, E. and Vermerris, W. *J. Appl. Polym. Sci.* **2015**, *132*, 42069.
29. Baumberger, S., Lapierre, C., Monties, B. and Valle, G. D. *Polym. Degrad. Stab.* **1998**, *59*, 273–277.
30. Mulder, W. J., Gosselink, R. J. A., Vingerhoeds, M. H., Harmsen, P. F. H. and Eastham, D. *Ind. Crop. Prod.* **2011**, *34*, 915–920.
31. Feng, Q., Cheng, H., Li, J., Wang, P. and Xie, Y. *BioRes.* **2014**, *9*, 3602–3612.
32. Spiridon, I., Leluk, K., Resmerita, A. M. and Darie, R. N. *Compos. Part B Eng.* **2015**, *69*, 342–349.
33. Norberg, I., Nordström, Y., Drougge, R., Gellerstedt, G. and Sjöholm, E. *J. Appl. Polym. Sci.* **2013**, *128*, 3824–3830.
34. Klapiszewski, Ł., Nowacka, M., Milczarek, G. and Jesionowski, T. *Carbohydrate Polym.* **2013**, *94*, 345–355.
35. Rong, H., Gao, B., Zhao, Y., Sun, S., Yang, Z., Wang, Y., Yue, Q. and Li, Q. *J. Environ. Sci.* **2013**, *25*, 2367–2377.

36. Wang, X., Zhang, Y., Hao, C., Dai, X., Zhoua, Z. and Si, N. *RSC Adv.* **2014**, *4*, 28156–28164.
37. He, W., Zhang, Y. and Fatehi, P. *Colloids Surf. A: Physicochem. Eng. Aspects* **2016**, *503*, 19–27.
38. Pintauer, T. and Matyjaszewski, K. *Chem. Soc. Rev.* **2008**, *37*, 1087–1097.
39. Matyjaszewski, K. and Xia, J. *Chem. Rev.* **2001**, *101*, 2921–2990.
40. Cheng, F.W. *Microchem. J.* **1952**, *3*, 537–542.
41. White, D.C. *Microchim. Acta.* **1961**, *49*, 449–456.
42. Plamper, F.A., Schmalz, A., Penott-Chang, E., Drechsler, M., Jusufi, A., Ballauff, M. and Müller, A.H.E. *Macromol.* **2007**, *40*, 5689–5697.
43. Xu, Y., Bolisetty, S., Drechsler, M., Fanf, B., Yuan, J., Ballauff, M. and Müller, A.H.E. *Polymer* **2008**, *49*, 3957–3964.
44. Gellerstedt, G., Gustafsson K. and Northey, R.A. *Nordic Pulp Pap. Res. J.* **1988**, *3*, 87–94.
45. Gellerstedt, G., Pranda, J. and Lindfors, E.-L. *J. Wood Chem. Technol.* **1994**, *14*, 467–482.
46. Ballauff, M. and Borisov, O. *Curr. Opin. Colloid Interface Sci.* **2006**, *11*, 316–323.
47. Das, S., Banik, M., Chen, G., Sinha, S., and Mukherjee, R., *Soft Matter*, **2015**, *11*, 8550–8583.

Tables

**Table 1** Reaction conditions, yield, molecular weights, Br amount, and molar ratio of Br to the KLBrB molecule of L100, L59, L22, and L0 samples

Sample code	BrBBr (mmol)	AcCl (mmol)	Yield (g)	$M_n/10^3$	$M_w/10^3$	Br amount (mmol/g-KLBrB)	Br/KLBrB (mol/mol)
L100	25.1	0	1.62	5.6	9.2	3.66	20.50
L59	18.9	6.4	1.18	-	-	2.57	12.02
L22	12.6	12.6	1.33	-	-	1.16	4.50
L0	0	25.2	0.78	3.4	5.7	0	0

**Table 2** Molar ratio between DMAEMA and Br, reaction conditions, conversions and yields of KLB-PDMAEMA and PDMAEMA samples

Sample code	Reaction conditions			Conversion (%)	Calculated DP <sub>s</sub>
	Molar ratio [DMAEMA]/[Br]	Monomer conc. (%)	Time (h)		
L100g39	73.3	33	72	53.2	39
L100g21	73.3	20	24	28.7	21
L100g03	73.3	10	24	4.7	3
L59g52	104.8	33	72	49.9	52
L59g30	104.8	20	24	28.8	30
L59g04	104.8	10	24	3.8	4
L22g94	229.2	33	72	40.9	94
L22g37	229.2	20	24	16.3	37
L22g05	229.2	10	24	2.0	5
g40	73.3	33	72	55.2	40

**Table 3** Results of elemental analysis of quaternized samples

Sample code	C (%)	H (%)	N (%)	N/C
qL100g39	36.02	6.06	4.33	0.120
qL100g21	35.08	6.21	4.13	0.118
qL100g3	37.35	6.46	3.93	0.105
qL59g52	34.19	6.40	4.12	0.121
qL59g30	35.25	6.36	4.19	0.119
qL59g4	38.68	6.56	3.79	0.098
qL22g94	34.80	6.05	4.22	0.121
qL22g37	35.57	6.42	4.08	0.115
qL22g5	40.89	6.47	3.58	0.087
qg40	35.45	6.20	4.58	0.129

## Figure captions

Figure 1 FT-IR spectra of KL, L100, L59, L22, and L0 samples.

Figure 2  $^{13}\text{C}$  NMR spectra of L100, L59, L22, and L0 samples in  $\text{CDCl}_3$ .

Figure 3  $^1\text{H}$  NMR spectrum of the L59g52 reaction solution in  $\text{CDCl}_3$ .

Figure 4  $^1\text{H}$  NMR spectra of L59g52 (a) before (in  $\text{CDCl}_3$ ) and (b) after (in  $\text{D}_2\text{O}$ ) quaternization reaction.

Figure 5 Results of dye removal test ( $n=3$ ): L22 series for (a) RBB, (b) DR, and (c) AB; L59 series for (d) RBB, (e) DR, and (f) AB; L100 series for (g) RBB, (h) DR, and (i) AB. Standard deviations were shown as error bars.

Figure 6 Schematic illustration of flocculation behavior between lignin-based star-shaped cationic flocculants and anionic dyes.

Figures

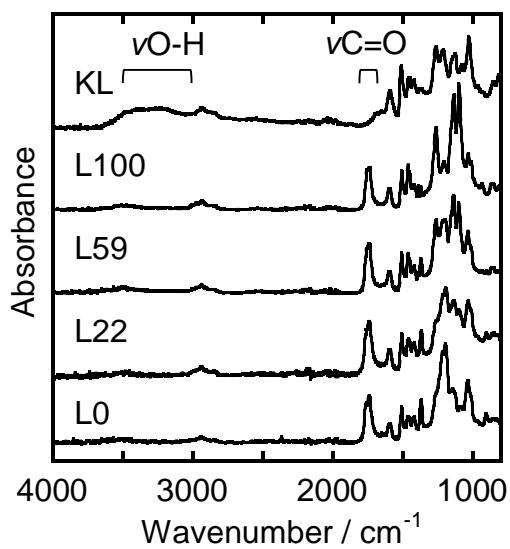


Figure 1 FT-IR spectra of KL, L100, L59, L22, and L0 samples.

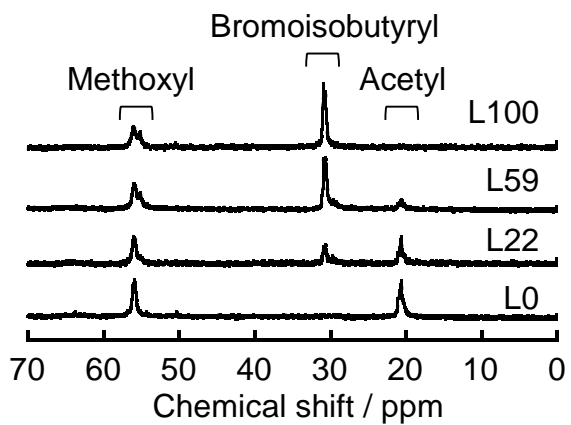


Figure 2 <sup>13</sup>C NMR spectra of L100, L59, L22, and L0 samples in CDCl<sub>3</sub>.

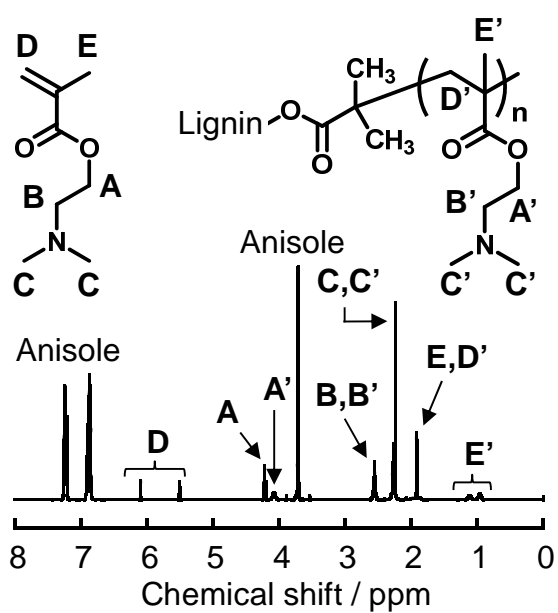


Figure 3  $^1\text{H}$  NMR spectrum of the L59g52 reaction solution for ATRP.

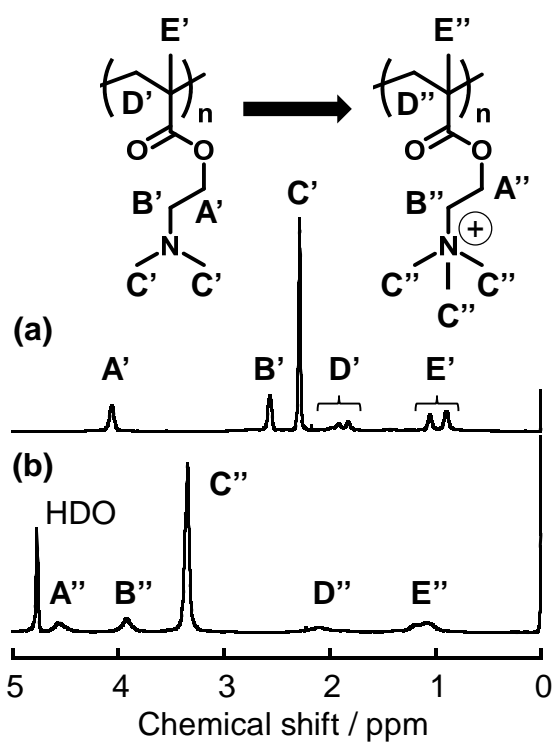


Figure 4  $^1\text{H}$  NMR spectra of L59g52 (a) before and (b) after quaternization reaction.

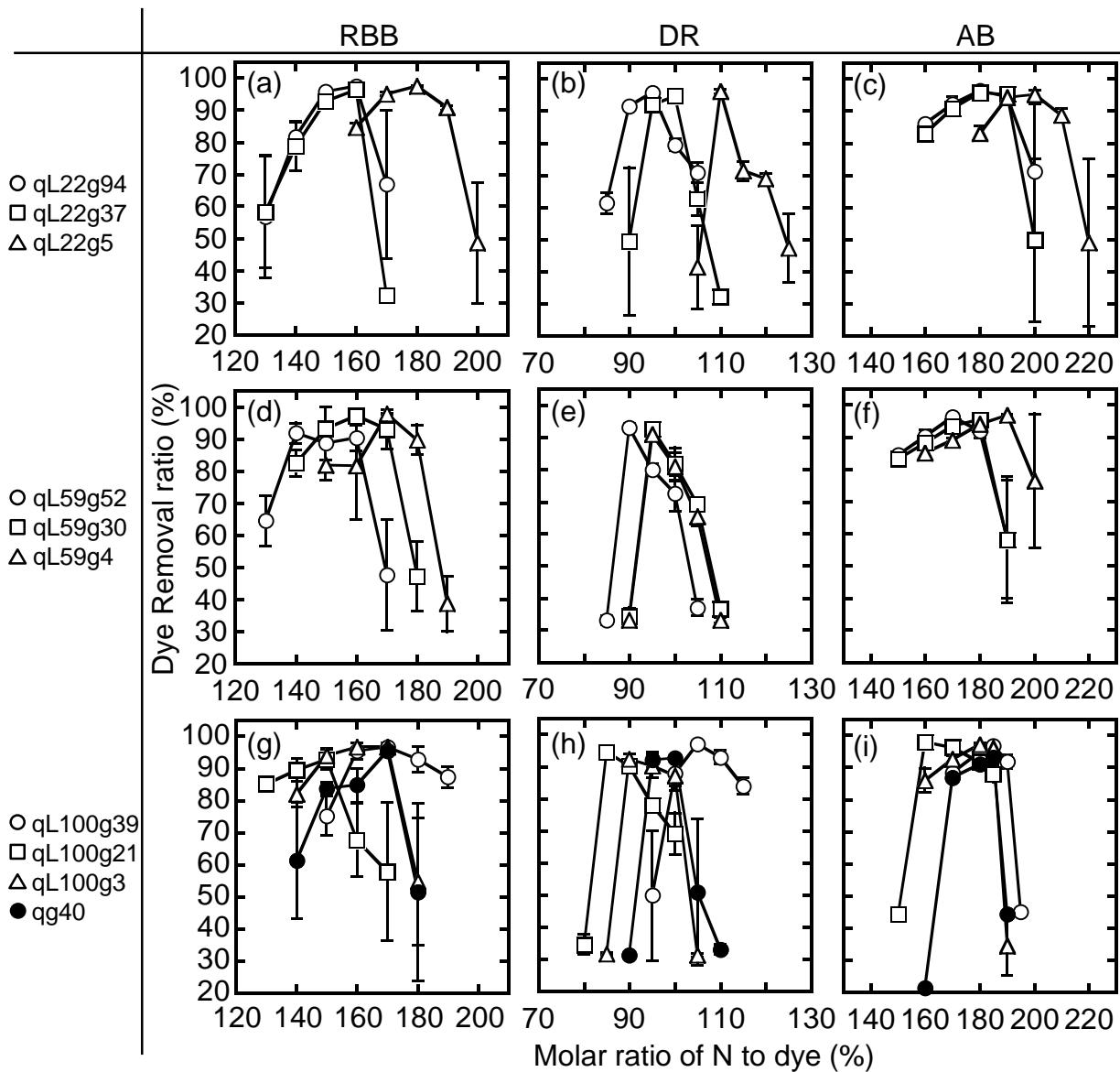


Figure 5 Results of dye removal test (n=3): L22 series for (a) RBB, (b) DR, and (c) AB; L59 series for (d) RBB, (e) DR, and (f) AB; L100 series for (g) RBB, (h) DR, and (i) AB. Standard deviations were shown as error bars.

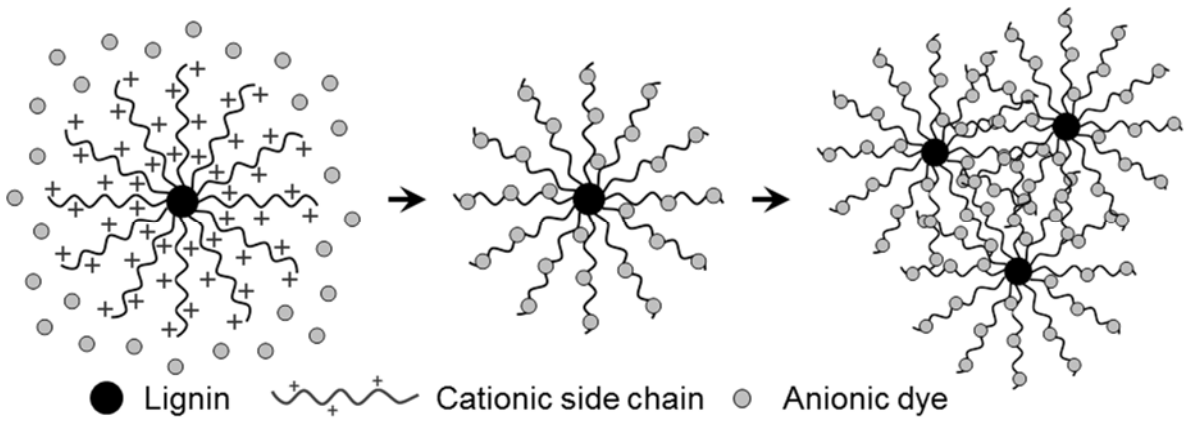


Figure 6 Schematic illustration of flocculation behavior between lignin-based star-shaped cationic flocculants and anionic dyes.